Green Chemistry

PAPER

View Article Online
View Journal | View Issue

Cite this: *Green Chem.*, 2015, **17**, 1589

Structural elucidation of whole lignin from *Eucalyptus* based on preswelling and enzymatic hydrolysis†

Jia-Long Wen, Shao-Long Sun, Tong-Qi Yuan and Run-Cang Sun*

The structural elucidation of whole lignin in the plant cell wall is extremely important for providing a representative lignin to understand the molecular characteristics of lignin in plants, and develop lignin-based polymers and green chemicals under the current biorefinery scenario. However, research in this area still lack methodologies for effectively isolating whole lignin from the plant cell wall. In this study, an effective method based on mild alkaline preswollen (4% NaOH, 25 °C, 24 h) and enzymatic hydrolysis for the isolation of "swollen residual enzyme lignin, SREL" from *Eucalyptus* wood was proposed. SREL was investigated as compared to the corresponding cellulolytic enzyme lignin (CEL) and alkali lignin (AL). Observably, the yield of SREL (95%) was significantly higher than that of the corresponding CEL (20%) and AL (12%). The isolated lignin has been comparatively investigated by a combination of elemental analysis, 2D HSQC NMR, ^{31}P-NMR, analytical pyrolysis, and GPC techniques. The major lignin linkages (β-O-4′, β–β′, β-5′, *etc.*) were thoroughly assigned and the frequencies of the major lignin linkages were quantitatively compared. Further experiments demonstrated that a transformation from cellulose I to cellulose II occurred during alkaline preswelling of the ball-milled Eucalyptus wood, which resulted in the efficient enzymatic hydrolysis of the substrates, thus yielding a representative lignin sample (SREL). However, the alkaline preswelling treatment has little effect on the lignin structures (typical substructures); it only tends to yield syringyl-rich lignin macromolecules as compared to CEL. Furthermore, the effective method gives us a panoramic image to understand the intrinsic structural features of whole lignin from other lignocellulosic biomasses and helps to develop more effective plant deconstruction or depolymerization strategies in the current biorefinery and catalytic conversion process.

Received 29th September 2014,
Accepted 8th December 2014

DOI: 10.1039/c4gc01889c

www.rsc.org/greenchem

1 Introduction

Lignin is the most abundant biopolymer in the plant cell wall besides cellulose, consisting primarily of three units: guaiacyl (G), sinapyl (S), and *p*-hydroxyphenyl (H) linked by aryl ether and carbon–carbon bonds. Located in the plant cell wall together with cellulose and hemicelluloses, lignin acts as a reinforcement for the lignocellulosic matrix. However, lignocellulosic materials are naturally resistant to microbial and enzymatic deconstruction, known as biomass recalcitrance.[1] Among the various factors affecting biomass deconstruction, the presence of lignin is one of the most significant contributors to biomass recalcitrance.[2] For many years, various pretreatments were developed to overcome biomass recalcitrance,[3] however, people still focus on the understanding of basic chemistry that is involved in the deconstruction process. Recently, some research studies demonstrated that ideal pretreatments to overcome biomass recalcitrance should maximize lignin removal or delocalization and minimize polysaccharide modification.[4,5]

Along with the research avenues for biomass deconstruction, the isolation and structural characterization of lignin has also been extensively investigated and developed in wood and lignin chemistry. Understanding the molecular structure of lignin obtained from the pretreatment and deconstruction processes is essential to tailoring the downstream conversion approach.[6,7] However, lignin molecules are extremely complicated due to their natural variability.[8] To date, the complex and irregular structure of lignin as well as the fundamental chemistry of lignin during the current biorefinery has not been completely elucidated although the primary structure has been well depicted.[9] Generally, it is of utmost importance to obtain a more representative lignin sample prior to the structural analysis of lignin in the plant cell wall. For this purpose,

Beijing Key Laboratory of Lignocellulosic Chemistry, Beijing Forestry University, Beijing, 100083, P. R. China. E-mail: rcsun3@bjfu.edu.cn; Fax: +86-10-62336903; Tel: +86-10-62336903

†Electronic supplementary information (ESI) available: Fig. S1–S10, Tables S1 and S2. See DOI: 10.1039/c4gc01889c

researchers have devoted their endeavours to find better isolation methods for structural analysis. The milled wood lignin (MWL) obtained is considered to be a representative source of native lignin and has been extensively used in the elucidation of the native lignin structure. Afterwards, cellulolytic enzyme lignin (CEL) was formally proposed.[10] Some improved methods to isolate CEL were subsequently brought forward.[11,12] CEL was found to be structurally similar to MWL, but in a higher yield, and hence it is more suitable for the structural analysis of native lignin in the plant cell wall. Recently, a novel effective procedure using the combination of enzymatic and mild acidolysis was proposed, and the obtained lignin preparation was named as enzymatic mild acidolysis lignin (EMAL).[13] The option for isolating lignin involves the use of ionic liquids.[14–16]

All the above-mentioned lignin preparations have played a very significant role in the structural elucidation of lignin in wood chemistry. However, these methods only focus on the isolated lignin fragments from the plant cell wall; also including some disadvantages, such as time-consuming and dissatisfactory yield of the lignin samples. Therefore, these methods could not provide panoramic structural features of whole lignin components *via* an un-isolated approach, *i.e.*, an *in situ* approach.

Recently, an *in situ* characterization of lignin in the plant cell wall by high-field solution-state NMR has been gradually achieved, which is useful in the rapid screening of biomass for bio-ethanol production and the pulping process.[17] Two-dimensional heteronuclear essential single quantum coherence (2D-HSQC) NMR spectroscopy of plant cell walls has been obtained by dissolving the modified or native ball-milled cell wall in deuterated solvents or mixtures, also called whole cell wall dissolution systems.[18–20] Generally, the acetylation of cell wall under mild conditions facilitates cell wall dissolution and thus achieves the NMR characterization of lignin in the plant cell wall.[18] However, a large number of carbohydrates undoubtedly impede the identification of the lignin signals and the quantification of these identified lignin structures. Another aspect is that the ball-milled plant cell wall was difficult to be completely dissolved in these dissolution systems.[19,20] In addition, some deuterated solvents (*e.g.* deuterated ionic liquid) were too expensive or unavailable although they have a good dissolving capacity for fine ball-milled plant cell wall.[21] These imperfections undoubtedly impede the direct NMR characterization of lignin in an *in situ* state. Moreover, from the perspective of structural analysis, more detailed structural features of lignin are needed to understand the native lignin based on a simple method. Thus, it is very important to find a universal method to obtain lignin for structural analysis although an ideal procedure for lignin isolation does not exist to date. Although the researchers are still looking for an ideal dissolution system of the plant cell wall for NMR characterization, the knowledge of these dissolution systems facilitates the development of new methods for lignin isolation. For example, the plant cell wall regenerated from a dissolution system (DMSO/NMI) has a higher enzymatic hydrolysis efficiency, which promotes CEL isolation.[12] Thus, it is important to find a pretreatment in which two premises should be satisfied simultaneously: (1) enhancing the enzymatic hydrolysis of the pretreated plant cell wall to remove most of the carbohydrates; (2) keeping the structure of lignin in the raw material unchanged as far as possible. Most publications demonstrated that enzymatic hydrolysis efficiency is related to the accessibility of cellulase to the pretreated substrates.[22–24] In addition, the swelling action of alkaline treatments also resulted in the changes in cellulose crystallinity and the crystallite size of pretreated biomass.[25] It was also reported that the XRD patterns of biomass were significantly changed after alkaline pretreatment under mild conditions, favoring the formation of cellulose II from cellulose I. In this case, the pretreated substrates were more readily digested than cellulose I.[22] Under these enlightenments, mild alkaline treatments and subsequent *in situ* enzymatic hydrolysis were applied to the ball-milled plant cell wall to remove carbohydrates as far as possible, obtaining swollen residual enzyme lignin (SREL) as the residual lignin, instead of extracting lignin with a neutral solvent (*i.e.* dioxane). Based on the above-mentioned enlightenments, a new paradigm of lignin isolation method from *Eucalyptus* wood was proposed for the first time. In addition, to evaluate the effect of mild alkaline treatments and enzymatic hydrolysis on the structural features of SREL, the corresponding alkaline lignin (AL) and cellulolytic enzyme lignin (CEL) isolated under the same conditions were used as the control.

In this study, the lignin preparation (SREL) obtained from the novel method was scientifically evaluated by comparing the yield, composition, and structural features with those of the corresponding CEL and AL. More importantly, quantitative information, including functional groups, syringyl/guaiacyl (S/G) ratio as well as major substructures (β-O-4′, β–β′ and β-5′), were obtained according to the elemental analysis, quantitative 2D-HSQC, and ^{31}P-NMR spectra and pyrolysis GC-MS. It is believed that the application of this method in biomass chemistry will enhance our understanding of the structural features of whole lignin in the plant cell wall.

2 Experimental

2.1 Material

Eucalyptus sawdust (2 × 0.5 × 0.5 cm) was prepared from *Eucalyptus grandis* × *Eucalyptus urophylla* wood (5 years old, harvested from Guangxi province, China). For the composition analysis, the sawdust (40–60 mesh) was extracted with toluene–ethanol (2 : 1, v/v) in a Soxhlet instrument for 6 h. The composition of Eucalyptus was 37.5% glucan, 16.2% xylan, 0.26% arabinan, 0.99% galactan, 32.3% Klason lignin, 2.0% acid-soluble lignin, which was analyzed by the standard of National Renewable Energy Laboratory (NREL).[26] The extractive-free Eucalyptus wood (30 g, 40–60 mesh) was ball-milled (5 h, 450 rpm) in a Fritsch planetary ball mill according to a previous publication.[27]

2.2 Preparation of swollen residual enzyme lignin (SREL)

The overall scheme for the isolation of swollen residual enzyme lignin (SREL) is presented in Fig. S1.† The ball-milled Eucalyptus powder was first slowly dissolved into 4% sodium hydroxide (1/25, g mL^{-1}) for 24 hour under stirring at room temperature (RT, 25 °C). After the preswollen process, the pH of the mixture was directly adjusted to 4.8 with acetic acid. The resulting mixtures were subjected to enzymatic hydrolysis, by loading large amounts of cellulase (50 FPU g^{-1}) and β-glucosidase (50 IU g^{-1}). The reaction mixture was incubated at 50 °C in a rotary shaker (200 rpm) for 48 h, afterward, the solution was centrifuged to remove the hydrolyzed carbohydrates, and the residue was named "swollen residual enzyme lignin (SREL)". The SREL was thoroughly washed with boiling water (pH = 2.0) to eliminate the residual enzymes and free sugars. Eventually, the purified SREL was freeze-dried.

2.3 Isolation of cellulolytic enzyme lignin (CEL) and alkali lignin (AL)

The isolation and purification of CEL was according to a previous publication,[10] while the alkali lignin (AL) was isolated from the ball-milled Eucalyptus powder (5 g) at room temperature for 24 h (solid to liquid ratio, 1 : 25; 4% NaOH) according to a previous publication with some modifications.[28] After the indicated period of time, the insoluble residue was collected by centrifugation, and washed repeatedly with distilled water. The supernatant fluid collected was re-filtered with Buchner funnel, neutralized to pH 5.5–6.0 with 6.0 M hydrochloric acid. Afterward, the neutral solution was concentrated by rotary evaporator. To remove alkali-extractable hemicelluloses prior to lignin isolation, the concentrated solution (50–60 mL) was poured into three volumes of 95% ethanol and precipitation (hemicelluloses) appeared. After centrifugation, the filtrate was concentrated to about 20–30 ml, and then the concentrated solution was dropped in acidic water (pH = 2.0) under stirring to induce lignin precipitation. The AL was washed with acidic water obtained after centrifugation (3000*g*, 30 min), and then freeze-dried.

2.4 Structure elucidation of the lignins

Elemental analysis of the lignins was carried out using an elemental analyzer Vario EL III (Elementar, Hanau, Germany). The oxygen content was deduced from the difference with respect to the total sample and the C_{900} formula of lignin was calculated. Carbohydrate analysis of lignin was conducted by hydrolysis with dilute sulfuric acid as previously reported.[26] Prior to molecular weight determination, the three lignin samples were acetylated as usual.[27] The weight average (M_w) and number-average (M_n) molecular weights of the three acetylated lignin samples were determined by gel permeation chromatography (GPC, Agilent 1200, USA) with an ultraviolet detector (UV) at 280 nm. The column used was a PL-gel 10 mm mixed-B 7.5 mm i.d. column, which was calibrated with PL polystyrene standards. Four milligrams of acetylated lignin was dissolved in 2 mL of tetrahydrofuran (THF), and 20 μL lignin solutions were injected by automatic sampler. The column was operated at ambient temperature and eluted with THF at a flow rate of 1.0 mL min^{-1}.

The NMR spectra were acquired on a Bruker Avance 400 MHz spectrometer fitted with a 5 mm gradient probe with inverse geometry (proton coils closest to the sample). The lignin sample (25 mg) was dissolved in 0.5 mL of DMSO-d_6. The central solvent peak at δ_C/δ_H 39.5/2.49 was used as an internal reference. The standard Bruker implementations of one- and two-dimensional (gradient-selected, ^{1}H-detected HSQC) NMR experiments were used for structural characterization and assignment authentication.[27,29] ^{31}P NMR spectra of lignin were conducted as previously reported, 20 mg lignin was dissolved in 500 μL of anhydrous pyridine and deuterated chloroform (1.6 : 1, v/v) under stirring. This was followed by the addition 100 μL of cyclohexanol (10.85 mg mL^{-1} in anhydrous pyridine and deuterated chloroform 1.6 : 1, v/v) as an internal standard and 100 μL of chromium(III) acetylacetonate solution (5 mg mL^{-1} in anhydrous pyridine and deuterated chloroform 1.6 : 1, v/v) as a relaxation reagent. The mixture was reacted with 100 μL of phosphitylating reagent (2-chloro-4,4,5,5-tetramethyl-1,3,2-dioxaphospholane, TMDP) for about 10 min and was transferred into a 5 mm NMR tube for subsequent NMR analysis.[30]

Analytical Py-GC/MS of the lignin recovered (approximately 100 μg) was performed with a CDS Pyroprobe 5200HP pyrolyser (Chemical Data Systems) connected to a Perkin Elmer GC/MS apparatus (Clarus 560) equipped with an Elite-35MS capillary column (30 × 0.25 mm i.d., 0.25 μm film thickness) according to previous publications.[31,32] Compounds were identified by comparing their mass spectra with the NIST library. The syringyl/guaiacyl (S/G) ratio was calculated by dividing the sum of peak areas from the syringyl units by the sum of peak areas of the guaiacyl derivatives of the selected markers, obtained by the integration of the peak areas and considering the total peak area as 100%. However, for most of the lignin derived phenols, the response factors were nearly identical, with the exception of vanillin, but this was a minor peak here.[32]

3 Results and discussion

3.1 Lignin isolation and its composition

One of the most used methods to isolate wood lignin for structural studies is the CEL method. The method uses cellulolytic enzyme mixtures (containing cellulases and hemicellulases) to remove most of the carbohydrates prior to lignin extraction with aqueous 1,4-dioxane. However, the yield of CEL is only 20% based on the Klason lignin of Eucalyptus wood in this study. Although the plant cell wall was ball-milled, the cellulose in plant cell walls is partly crystalline (Fig. S2†), with a high degree of polymerization, and also embedded in a matrix of wood polysaccharides and lignin, it is highly inaccessible to enzymatic attack.[23,24] It was reported that the dissolution or swelling of cellulose by solvents was considered to be a more facile method for disrupting the crystalline structure to

increase its accessibility to cellulases.[11,12] In this study, the aqueous sodium hydroxide was used for the preswelling and dissolution of the ball-milled wood. The wood sample could be mostly dissolved after stirring for 24 h at room temperature. After treatment with crude cellulase, the mass losses for the original and pretreated ball-milled wood were 60.0% and 70.0%, respectively. These results suggested that the digestibility of cellulose (and other polysaccharides) by cellulases was significantly improved after preswelling and dissolution in aqueous sodium hydroxide. The greatly enhanced efficiency of enzymatic hydrolysis of the preswelled ball-milled wood was primarily ascribed to the changed crystallization morphology of the substrate in a sodium hydroxide solution.[24] It was also found that the preswelling ball-milled wood exhibited a typical XRD pattern of cellulose II (Fig. S2†), suggesting that a transformation from cellulose I to cellulose II occurred during alkaline swelling, with their representative Miller indices for the reflections (1−10), (110), and (020) for cellulose II at 12.8°, 20.2°, and 22.0°, respectively.[22] In addition, the removal or delocalization of lignin and hemicelluloses from the surface of the substrate by a mild alkaline treatment enhanced the enzymatic hydrolysis of the pretreated substrates.[4,33] SEM images also showed that the untreated ball-milled wood had a rigid and compact morphology, whereas the surface morphology of the preswelling wood exhibited a rough and loosened structure as a result of the removal of lignin and hemicelluloses from the substrates (Fig. S3†). More importantly, it was found that the swollen residual enzyme lignin (SREL), obtained after the enzymatic hydrolysis of wood pretreated with a sodium hydroxide solution, could be directly dissolved in DMSO-d_6 in this study; by contrast, the residue obtained after the enzymatic hydrolysis of the original ball-milled wood only partially dissolved in DMSO-d_6 (Fig. S4†). This finding facilitates us to characterize the structural features of SREL directly by NMR technique, rather than extracting CEL with 96% dioxane for further NMR characterization. To evaluate the potential chemical and structural transformations of lignin brought about by the preswelling treatments, the structural features and quantitative information of the corresponding CEL and CEL-AL have been investigated by NMR and it was found that the mild alkaline treatment applied has a slight effect on their lignin structures (Table S1 and Fig. S5 and the related discussions could be found in ESI†). Considering the highest yield of SREL (95%), SREL was an ideal lignin sample for structural analysis. Surprisingly, after evaluating the associated carbohydrate contents in these lignin samples, it was found that SREL contained a small quantity of associated sugars (8.70%, w/w), while CEL and AL contained 13.40% and 0.30% sugars based on dry lignin (w/w), respectively (Table 1). In light of the results obtained (super-high yield and low associated sugars), it was concluded that SREL can better represent whole lignin in the plant cell wall. After carefully examining the composition of the associated carbohydrates, it was observed that glucose was the major sugar in SREL, while xylose was the major sugar in CEL. The differences between the associated sugars could be attributed to the different isolating methods,

Table 1 Yields, carbohydrate contents and C_{900} formulae of lignin preparations

Sample	SREL	CEL	AL
Yield[a]	95%	20%	12%
Carbohydrate	8.70%	13.40%	0.30%
Arabinose	1.39%	0.95%	N.D.
Galactose	1.30%	0.76%	N.D.
Glucose	3.73%	3.26%	0.24%
Xylose	0.92%	7.95%	0.16%
Mannose	1.36%	0.48%	N.D.[b]
C%	57.04	59.16	59.10
H%	6.27	6.23	5.95
O%	34.85	34.61	34.95
N%	1.84	N.D.	N.D.
OCH_3 (%)	20.97	20.66	21.25
C_{900} formula	$C_{900}H_{935}O_{332}(OCH_3)_{150}$	$C_{900}H_{895}O_{316}(OCH_3)_{139}$	$C_{900}H_{823}O_{316}(OCH_3)_{146}$

[a] The yield is calculated based on the Klason lignin. [b] N.D., not detected.

e.g. the higher content of glucose is related to the small amount of obstinate cellulose in SREL, while the abundant xylose is ascribed to the potential lignin–carbohydrate complex (LCC), in agreement with a previous publication.[29] The elemental composition and methoxy group (OMe) contents of the lignin samples, together with the calculated approximate C_{900} formulas, are also listed in Table 1. As shown in the C_{900} formulas, the OMe contents in SREL and AL are higher than that of CEL. The numbers of oxygen are 332, 316, and 316/C_{900} and those of OMe groups are 150, 139, and 146/C_{900} in SREL, CEL, and AL, respectively. It is known that higher oxygen contents in lignins approximating the theoretical limit of 300/C_{900} (or above) are indicative of carbohydrate residues originating from the lignin–carbohydrate linkages, implying that the associated carbohydrates in these lignin are potentially originated from LCC linkages. However, the oxygen content of lignins could be elevated by the large amounts of carboxylic group, which result from alkaline treatment.

3.2 2D-HSQC spectra analysis

To investigate the composition and detailed chemical structures of the lignin obtained, the lignin samples (SREL, CEL, and AL) were analyzed using the 2D HSQC NMR technique. The main structural characteristics of lignins, including basic composition (S, G, and H units) and various substructures linked by ether and carbon–carbon bonds (β-O-4′, β–β′, β-5′, *etc.*), can be observed in the 2D HSQC spectra. The side-chain and aromatic regions of 2D HSQC spectra are shown in Fig. 1 and the main substructures are depicted in Fig. S8.† In the side-chain region of the spectra of Eucalyptus lignin samples, the substructures, such as β-O-4′ aryl ethers (A), resinols (B), phenylcoumarans (C), could be easily assigned according to the previous publications.[27,34,35] All the spectra showed prominent signals corresponding to β-O-4′ ether units (substructure A). The C_α–H_α correlations in the β-O-4′ linkages were observed at δ_C/δ_H 72/4.7 to 4.9, while the C_β–H_β correlations were observed at δ_C/δ_H 84/4.3 and 86/4.1 for the substructures

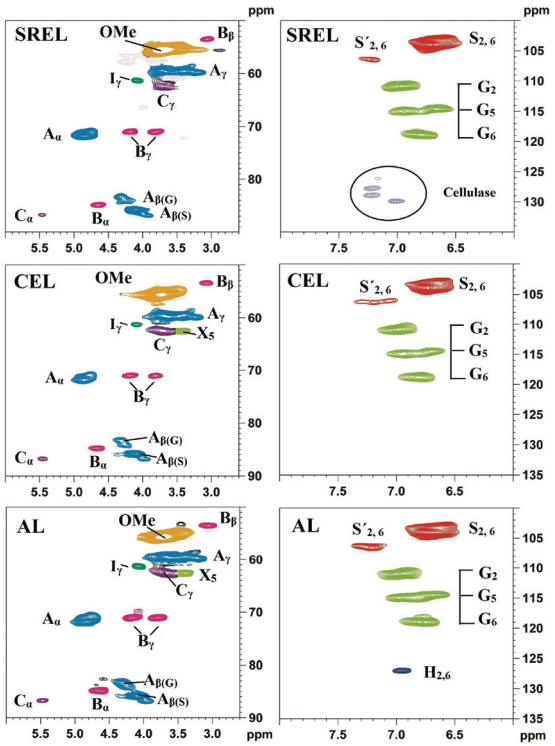

Fig. 1 Side-chain and aromatic region in the 2D HSQC NMR spectra of the lignins.

linked to the G and S units, respectively. The C_γ–H_γ correlations in the β-O-4′ substructures were found at δ_C/δ_H 60.1/3.40 and 3.72, partially overlapped with other signals, such as C_5–H_5 of the associated xylans (especially in CEL). In addition to the abundant β-O-4′ linkages, resinol (β–β′, substructures B) appeared in the spectra in noticeable amounts as indicated by their C_α–H_α, C_β–H_β, and the double C_γ–H_γ correlations at δ_C/δ_H 84.8/4.66, 53.5/3.07, 71.2/3.82 and 4.18, respectively. Phenylcoumaran (β-5′, substructures C) was also detected in a minor amount. Moreover, a trace amount of the spirodienone substructure (β-1′, substructures D) was also detected (not shown in the contour level, shown in Fig. S6†). Furthermore, the signal located at δ_C/δ_H 62/4.1 was assigned to the C_γ–H_γ correlation of *p*-hydroxycinnamyl alcohol end groups (I).

Besides the substructure linkages observed, benzyl ether (BE) LCC structures were also mainly detected in CEL, while SREL and AL exhibited less BE LCC signals, suggesting that BE (LCC) linkages are not stable under the given alkaline conditions.

In the aromatic region of HSQC spectra, signals from the syringyl (S) and guaiacyl (G) units were clearly distinguished. The S-units showed an obvious signal for the $C_{2,6}$–$H_{2,6}$ correlations at δ_C/δ_H 103.5/6.66, while the signals for the C_α-oxidized S-units (S′) were observed at δ_C/δ_H 106.3/7.32. By contrast, three different cross-signals were assigned to G-units: C_2–H_2 (δ_C/δ_H 110.8/6.97), C_5–H_5 (δ_C/δ_H 114.5/6.70 and 115.1/6.95), and C_6–H_6 (δ_C/δ_H 119.0/6.78). Interestingly, the $C_{2,6}$–$H_{2,6}$ correlations in H unit appeared in a lower amount at δ_C/δ_H 127.0/6.95 in AL rather than in CEL. Although SREL also exhibited three signals near the H units, these signals were mainly originated from residual cellulase by subsequent NMR analysis (Fig. S7†).

3.3 Summary of changes in the lignin structure as revealed by quantitative 2D-HSQC NMR spectra

The relative abundances of the basic composition (H, G, and S lignin units), and those of the main linkages (referred to as per 100 aromatic units and as a percentage of the total side chains), calculated from the 2D HSQC spectra of the lignin samples based on a previous publication,[34] are shown in Table 2. The S/G ratio is important to reveal the top-chemistry of the lignin isolation and delignification process. In this study, the S/G ratio of CEL is 1.42, which is lower than that of the corresponding SREL (1.60) and AL (1.67). Although both SREL and AL have a higher S/G ratio than CEL, different reasons are accounted for the respective higher S/G ratio of SREL and AL. For SREL, the higher S/G ratio can better represent the basic composition of Eucalyptus wood. One should be aware that the S/G ratio obtained is an average value of the lignin originated from different parts of the plant cell wall, such as the middle lamella (ML) and the S2 layer of the secondary wall (S2). The ML was reported to contain more G-type units and S2 has more S-type lignin units.[36] However, the higher S/G ratio of AL suggested that the S-rich lignin fragment was more easily released than the G-rich lignin under alkaline conditions. Similarly, it was reported that the S-rich lignin units could be easily reacted, resulting in the easy delignification under alkaline conditions at different temperatures.[37] Another reason for the high S/G ratio of AL was related to the good reactivity of alkaline solutions to non-condensed lignin, and the fine permeability of alkaline solutions to the S2 layer of the plant cell wall. It was potentially possible that the alkaline solution first permeates into most of the plant cell wall, dissolves and removes hemicelluloses in the S2 layer, and cleaves the potential LCC bonds, thus facilitating the dissolution of lignin in the S2 layer. In addition to the S- and G-type lignin, it was noted that a small quantity of the H-type lignin units occurred in AL. It was reported that the H-type lignin units were deposited in the cell wall very early in the lignification process and may therefore be associated with the initiation of lignification.[38] Thus, the signal located at 127.5/6.95 ppm in AL was attributable to the appearance of H-type lignin units, but the nature and origin of the H units still needs to be confirmed.

Table 2 Quantification of the lignins by quantitative 2D-HSQC method: results expressed per 100 Ar (and as percentage of total side chains)

Sample	β-O-4′	β–β′	β-5′	S/G
SREL	53.6 (81.1)	9.3 (15.1)	1.5 (3.8)	1.60
CEL	55.3 (75.7)	12.0 (17.6)	4.0 (6.7)	1.42
AL	55.5 (78.4)	13.3 (18.8)	2.0 (2.8)	1.67

With respect to the relative content of different linkage types (in parentheses), all the lignin samples display a predominance of the β-O-4′ aryl ether units (A, 75.7%–81.1% of total side chains) followed by the β–β′ resinol-type units (B; 15.1%–18.8%) and lower amounts of the β-5′ phenylcoumaran-type (C; 2.8%–6.7%). It was observed that the relative content of the β-O-4′ linkages is higher in SREL and AL, probably resulting from the abundant S-type lignin units in these lignin samples. Basically, monolignol addition to a syringyl unit has essentially only a single pathway available, the β-O-4′ linkage.[20] In contrast, the abundance of phenylcoumaran structures decreased in the order of CEL > SREL > AL, which is most probably related to the decrease in G lignin observed in these lignin samples. That is, β-5′ can only be obtained from the coupling of a monolignol with a guaiacyl (G) or a *p*-hydroxyphenyl (H) unit.[20] By contrast, the abundances per aromatic unit of β-O-4′ in SREL seemed to be decreased although the relative content of β-O-4′ is the highest in these lignin samples, which is probably related to the SREL itself, because SREL is not an extracted lignin, but a residual lignin. Similarly, the same phenomenon was observed in a previous publication, in which slightly lower abundances per aromatic unit were also found in the whole cell wall NMR spectra.[39] In short, SREL was found to be an ideal lignin sample to characterize whole lignin in the plant cell wall for considering its typical structural features and considerable yield.

3.4 ^{31}P-NMR spectra

To further evaluate the functional groups of lignin samples, quantitative ^{31}P NMR technique was also applied.[30] The spectra of the lignins are shown in Fig. 2 and the corresponding results are listed in Table 3. For SREL, CEL, and AL, the content of S-type OH was less than that of the corresponding G-type OH, as revealed by the S/G ratio calculated from the ^{31}P-NMR spectra. This suggested that most of the S-type lignin unit is involved in the formation of the β-O-4′ linkage in these lignins and only a small amount of free S-OH could be detected by the ^{31}P-spectra. Generally, the cleavage of β-aryl ether linkages gives rise to phenolic hydroxyl groups, while oxidation reactions may result in the oxidative fragmentation of the lignin macromolecule with the concomitant creation of a carboxylic acid group.[40] Less amount of phenolic OH in SREL than in CEL suggests that SREL probably contains more etherified lignin units, that is, phenolic OH is linked as β-O-4′ linkages and phenyl glycoside linkages.[30] However, the contents of COOH in SREL and AL were abundant as compared to that of CEL. This is probably attributable to the cleavage of the potential LCC linkages (Fig. S6†), thus releasing more glucuronic acid during alkaline treatment. In addition, the existence of carbohydrates in CEL also elevates the amount of aliphatic OH in CEL, as revealed by the higher content of carbohydrates (Table 1).[41,42] Moreover, non-condensed H-type phenolic OH was found in AL and SREL rather than in CEL, demonstrating the existence of H-type lignin units in AL.

Table 3 Quantification of the functional groups in the lignins by quantitative ^{31}P-NMR method

Samples	SREL	CEL	AL
Aliphatic-OH	3.74	5.23	2.90
Condensed S-OH	0.07	0.02	0.02
Non-condensed S-OH	0.12	0.24	0.17
Condensed G-OH	0.03	0.05	0.04
Non-condensed G-OH	0.18	0.43	0.27
Non-condensed H-OH	0.01	N.D.	0.03
COOH	0.13	0.03	0.19
S/G ratio (phenolic-OH)	0.90	0.54	0.61

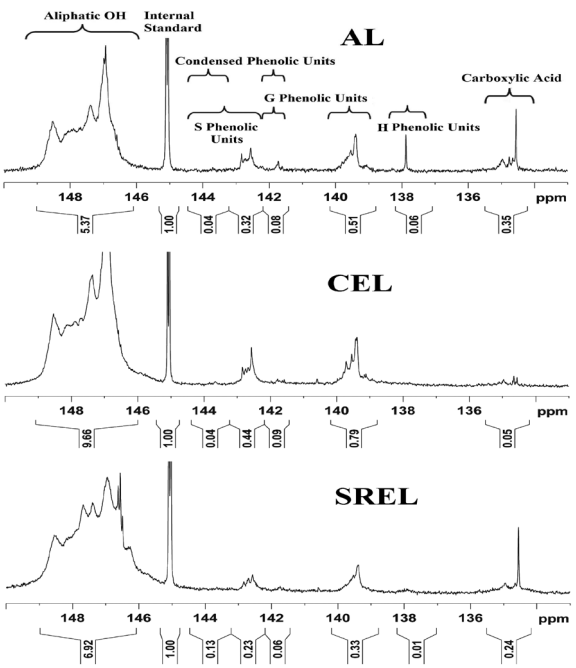

Fig. 2 Quantitative ^{31}P NMR spectra of the lignins.

3.5 Molecular weights

Fig. 3 shows the curves of weight-average (M_w) and number-average (M_n) molecular weights and the polydispersity index (PDI, M_w/M_n) of the lignin samples obtained from Eucalyptus

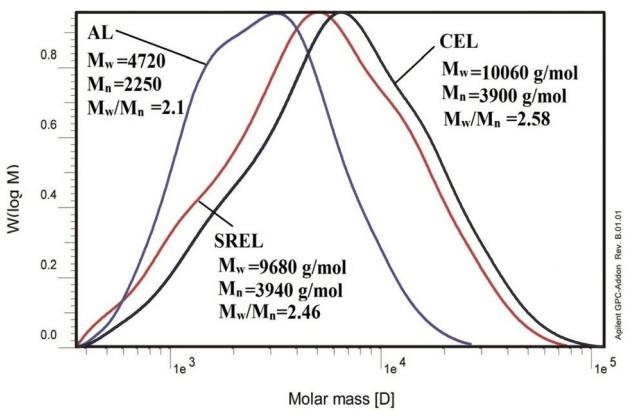

Fig. 3 GPC curves of the lignins.

wood. It was found that CEL has a higher M_w than that of AL and SREL; however, the highest M_w of CEL is probably related to the associated carbohydrates.[43] By contrast, considering the molecular weight, and higher β-O-4′ linkages, and less phenolic OH of SREL, it was concluded that the proposed lignin isolating method could serve as an effective method to prepare lignin samples for structural analysis.

3.6 Pyrolysis-gas chromatography/mass spectrometry of the isolated lignin polymers

The Py-GC/MS chromatograms of the lignin samples are shown in Fig. S9† and the detected lignin-degradation products are listed in Fig. S10.† The identities and relative abundances of the released compounds are listed in Table S2.† Among them, guaiacyl (G) and syringyl-type (S) phenols were identified. Only minor amounts (2%) of phenol-type compounds from *p*-hydroxyphenyl (H) units could be detected. The most important compounds identified were phenol, 4-methoxy-, acetate (peak 4), 1,2-benzenediol, 3-methoxy (peak 7), 2-methoxy-4-vinylphenol (peak 10), phenol,2,6-dimethoxy- (peak 12), 1,2,4-trimethoxy-benzene (peak 18), 3′,5′-dimethoxy-acetophenone (peak 25), phenol, 2,6-dimethoxy-4-(2-propenyl) (peak 33).

Py-GC/MS has been successfully used to analyze the relative S/G ratio of lignin.[32] The syringyl/guaiacyl (S/G) ratios of the lignins obtained from different methods are shown in Table S2.† In all samples, the S-type and G-type degradation products were released in different amounts, with an S/G ratio ranging from 0.86 (CEL) to 1.01 (AL). For example, SREL showed a higher S/G ratio as compared to the corresponding CEL (Table S2†), which was in line with the 2D-HSQC results aforementioned. However, as compared to the highest S/G ratio of AL, the moderate S/G ratio of SREL suggested that some S-type lignin was degraded and removed during the SREL isolation process. Another aspect is that although the S/G ratio of the lignin obtained from Py-GC/MS is lower than the corresponding value acquired by 2D-HSQC NMR results, the overall trend of the S/G ratio is consistent. The differences of S/G ratios were probably related to the demethoxylation induced by the pyrolysis process. In addition, the demethoxylation of syringyl units occurred more easily than that of G units during the pyrolysis process, thus leading to the formation of more guaiacyl-type degradation products and decreasing the S/G ratio.[44]

3.7 Implications

Eucalyptus lignin is typical hardwood lignin (GS type lignin) according to the previous publications,[32,34] without some sensitive structures, such as acetylation, *p*-coumarate esters (PCE),[39] and *p*-hydroxybenzoate substructures (PB).[45] In fact, "SREL" was also obtained with high yield and acceptable purity from other plants with sensitive structures, such as poplar wood and transgenic poplars (unpublished data). To obtain a more purified lignin sample, further treatment of lignin with protease is feasible. In addition, NMR results showed that a part of the *p*-hydroxybenzoate substructures (PB) in these "SREL" samples has been cleaved during the alkaline preswelling process. However, the vast majority of typical substructures (β-O-4′, β–β′, and β-5′) have been well reserved, highly similar to that of the corresponding CEL, suggesting that the applicability of this method in the structural characterization of lignin is favourable. Further NMR analysis of lignin before and after the alkaline preswelling also indicated that preswelling has a slight effect on the composition and chemical structures of lignin. Therefore, lignin samples obtained by this method from different biomasses can be used for a better characterization of the structural features of lignins in these plants as compared to the currently well-accepted lignin preparations.

4 Conclusions

It has been illustrated that the preswelling/dissolution pretreatment with sodium hydroxide significantly improves enzymatic hydrolysis of polysaccharides in ball-milled wood, thus increasing the yield and purity of the residual lignin (SREL). SREL was demonstrated to be an ideal sample to characterize the structural features of lignin in most lignocellulosic materials. The data presented in this study indicated that mild alkaline treatment has a slight effect on the native lignin structures, and the lignin obtained by this method is syringyl-rich lignin, having more abundant β-O-4′ linkages and less phenolic hydroxyl groups. A comparison of the CEL, AL, and SREL preparations using various analysis approaches, revealed that all these samples have similar chemical compositions and structural features. To the best of our knowledge, this is the first time that the method has been presented in the literature. Surprisingly, this method also gives some inspirations for a better deconstruction of the plant cell wall in an easy approach, which is crucial to the pretreated process in the current biorefinery process. Another, the representative lignin fraction (SREL) can be used as a lignin model to investigate the chemical transformations and the depolymerization of lignin under a biorefinery and green chemistry scenario.

Acknowledgements

This work was supported by the grants from the Fundamental Research Funds for the Central Universities (BLX2014-37), National Natural Science Foundation of China (31110103902, 31430092, and 31400296).

References

1 M. E. Himmel, S.-Y. Ding, D. K. Johnson, W. S. Adney, M. R. Nimlos, J. W. Brady and T. D. Foust, *Science*, 2007, **315**, 804–807.
2 T. Q. Yuan, F. Xu and R. C. Sun, *J. Chem. Technol. Biotechnol.*, 2013, **88**, 346–352.

3 X. Zhao, L. Zhang and D. Liu, *Biofuel Bioprod. Biorefin.*, 2012, **6**, 561–579.
4 S. Y. Ding, Y. S. Liu, Y. Zeng, M. E. Himmel, J. O. Baker and E. A. Bayer, *Science*, 2012, **338**, 1055–1060.
5 Y. Zeng, S. Zhao, S. Yang and S. Y. Ding, *Curr. Opin. Biotechnol.*, 2014, **27**, 38–45.
6 N. Sathitsuksanoh, K. M. Holtman, D. J. Yelle, T. Morgan, V. Stavila, J. Pelton, H. Blanch, B. A. Simmonsa and A. George, *Green Chem.*, 2014, **16**, 1236–1247.
7 T. M. Jarrell, C. L. Marcum, H.-m. Sheng, B. C. Owen, C. J. O'Lenick, H. Maraun, J. J. Bozell and H. I. Kenttämaa, *Green Chem.*, 2014, **16**, 2713–2727.
8 S. Nanayakkara, A. F. Patti and K. Saito, *Green Chem.*, 2014, **16**, 1897–1903.
9 J. Ralph, K. Lundquist, G. Brunow, F. Lu, H. Kim, P. F. Schatz, J. M. Marita, R. D. Hatfield, S. A. Ralph and J. H. Christensen, *Phytochem. Rev.*, 2004, **3**, 29–60.
10 H. M. Chang, E. B. Cowling and W. Brown, *Holzforschung*, 1975, **29**, 153–159.
11 J. Y. Chen, Y. Shimizu, M. Takai and J. Hayashi, *Wood Sci. Technol.*, 1995, **29**, 295–306.
12 A. P. Zhang, F. Lu, R. C. Sun and J. Ralph, *J. Agric. Food Chem.*, 2010, **58**, 3446–3450.
13 S. Wu and D. Argyropoulos, *J. Pulp Pap. Sci.*, 2003, **29**, 235–240.
14 N. Sun, M. Rahman, Y. Qin, M. L. Maxim, H. R. Rodriguez and D. Rogers, *Green Chem.*, 2009, **11**, 646–655.
15 A. Pinkert, D. F. Goeke, K. N. Marsh and S. S. Pang, *Green Chem.*, 2011, **13**, 3124–3136.
16 S. S. Y. Tan, D. R. MacFarlane, J. Upfal, L. A. Edye, W. O. S. Doherty, A. F. Patti, J. M. Pringle and J. L. Scott, *Green Chem.*, 2009, **11**, 339–345.
17 F. Lu and J. Ralph, *J. Biobased Mater. Bioenergy*, 2011, **5**, 169–180.
18 F. Lu and J. Ralph, *Plant J.*, 2003, **35**, 535–544.
19 H. Kim, J. Ralph and T. Akiyama, *Bioenergy Res.*, 2008, **1**, 56–66.
20 H. Kim and J. Ralph, *Org. Biomol. Chem.*, 2010, **8**, 576–591.
21 K. Cheng, H. Sorek, H. Zimmermann, D. E. Wemmer and M. Pauly, *Anal. Chem.*, 2013, **85**, 3213–3221.
22 T. Q. Yuan, W. Wang, F. Xu and R. C. Sun, *Bioresour. Technol.*, 2013, **144**, 429–434.
23 V. Arantes and J. N. Saddler, *Biotechnol. Biofuels*, 2010, **3**, 4–11.
24 X. Zhao, L. Zhang and D. Liu, *Biofuel Bioprod. Biorefin.*, 2012, **6**, 465–482.
25 A. Mittal, R. Katahira, M. E. Himmel and D. K. Johnson, *Biotechnol. Biofuels*, 2011, **4**, 1–16.
26 A. Sluiter, B. Hames, R. Ruiz, C. Scarlata, J. Sluiter, D. Templeton and D. Crocker, Laboratory Analytical Procedure (NERL), 2008.
27 J. L. Wen, T. Q. Yuan, S. L. Sun, F. Xu and R. C. Sun, *Green Chem.*, 2014, **16**, 181–190.
28 R. C. Sun, J. M. Lawther and W. B. Banks, *J. Agric. Food Chem.*, 1996, **44**, 3965–3970.
29 J. L. Wen, S. L. Sun, B. L. Xue and R. C. Sun, *J. Agric. Food Chem.*, 2013, **61**, 635–645.
30 A. Granata and D. S. Argyropoulos, *J. Agric. Food Chem.*, 1995, **43**, 1538–1544.
31 L. P. Xiao, Z. J. Shi, F. Xu and R. C. Sun, *Bioenergy Res.*, 2013, **6**, 519–532.
32 J. Rencoret, A. Gutiérrez, L. Nieto, J. Jiménez-Barbero, C. B. Faulds, H. Kim, J. Ralph, Á. T. Martínez and C. José, *Plant Physiol.*, 2011, **155**, 667–682.
33 H. Yang, Q. Chen, K. Wang and R. C. Sun, *Bioresour. Technol.*, 2013, **147**, 539–544.
34 J. Rencoret, G. Marques, A. Gutierrez, D. Ibarra, J. Li, G. Gellerstedt, J. I. Santos, J. Jiménez-Barbero, A. T. Martinez and J. C. del Río, *Holzforschung*, 2008, **62**, 514–526.
35 J. L. Wen, S. L. Sun, B. L. Xue and R. C. Sun, *Materials*, 2013, **6**, 359–391.
36 P. Whiting and D. Goring, *Wood Sci. Technol.*, 1982, **16**, 261–267.
37 S. Shimizu, T. Yokoyama, T. Akiyama and Y. Matsumoto, *J. Agric. Food Chem.*, 2012, **60**, 6471–6476.
38 J. Ralph, T. Akiyama, H. Coleman and S. Mansfield, *Bioenergy Res.*, 2012, **5**, 1009–1019.
39 J. L. Wen, B. L. Xue, F. Xu and R. C. Sun, *Bioenergy Res.*, 2012, **5**, 886–903.
40 A. Guerra, L. A. Lucia and D. S. Argyropoulos, *Holzforschung*, 2008, **62**, 24–30.
41 H. Sadeghifar, J. P. Dickerson and D. S. Argyropoulos, *Carbohydr. Polym.*, 2014, **113**, 552–560.
42 Y. Q. Pu, S. L. Cao and A. J. Ragauskas, *Energy Environ. Sci.*, 2011, **4**, 3154–3166.
43 A. Jääskeläinen, Y. Sun, D. Argyropoulos, T. Tamminen and B. Hortling, *Wood Sci. Technol.*, 2003, **37**, 91–102.
44 P. F. van Bergen, I. Poole, T. Ogilvie, C. Caple and R. P. Evershed, *Rapid Commun. Mass Spectrom.*, 2000, **14**, 71–79.
45 T. Q. Yuan, S. N. Sun, F. Xu and R. C. Sun, *J. Agric. Food Chem.*, 2011, **59**, 6605–6615.

